Journal of Materials Processing Technology xxx (2010) xxx–xxx

Contents lists available at ScienceDirect

Journal of Materials Processing Technology

journal homepage: www.elsevier.com/locate/jmatprotec

Pulsed Nd:YAG laser seam welding of AISI 316L stainless steel thin foils

Vicente Afonso Ventrella[a,*], José Roberto Berretta[b], Wagner de Rossi[b]

[a] Universidade Estadual Paulista-UNESP, Departamento de Engenharia Mecânica, Av. Brazil Centro-56, 15.385-000, Ilha Solteira, SP, Brazil
[b] Instituto de Pesquisas Energéticas e Nucleares-IPEN, Centro de Lasers e Aplicações, P.O. Box 11049, São Paulo, SP, Brazil

ARTICLE INFO

Article history:
Received 14 October 2009
Received in revised form 27 April 2010
Accepted 24 June 2010
Available online xxx

Keywords:
Welding
Nd:YAG laser
Stainless steel
Thin foil
Microhardness
Tensile shear strength

ABSTRACT

Experimental investigations were carried out using a pulsed neodymium:yttrium aluminum garnet laser weld to examine the influence of the pulse energy in the characteristics of the weld fillet. The pulse energy was varied from 1.0 to 2.25 J at increments of 0.25 J with a 4 ms pulse duration. The base material used for this study was AISI 316L stainless steel foil with 100 μm thickness. The welds were analyzed by optical microscopy, tensile shear tests and microhardness. The results indicate that pulse energy control is of considerable importance to thin foil weld quality because it can generate good mechanical properties and reduce discontinuities in weld joints. The ultimate tensile strength of the welded joints increased at first and then decreased as the pulse energy increased. The process appeared to be very sensitive to the gap between couples.

1. Introduction

In general, one important problem in the experimental measurements performed at elevated temperatures or in a corrosive environment is selecting a material that is resistant to chemical attack and is easily formed into the desired shape. For this purpose, industrial product parts and components are covered with stainless steel thin foils or other corrosion-resistant material such as tantalum and Ni alloys. The significance of microtechnology has increased dramatically over the last years, and this has created a growing need for microwelding of thin foils. Furthermore, Nd:YAG pulsed laser welding is expected to be the method of choice because it allows more precise heat control compared with others processes and it reduces the heat-affected zone (HAZ), residual stress and the presence of discontinuities.

Materials play an important role in manufactured goods. Materials must possess both acceptable properties for their intended applications and manufacturability. These criteria hold true for micromanufacturing, in which parts have overall dimensions of less than 1 mm. The wide range of materials that can be processed by lasers includes materials for micro-electronics, hard materials such as tungsten carbide for tool technology and very weak and soft materials, such as polymers for medical products. Even ceramics, glass and diamonds can be processed with laser technology to an accuracy better than 10 μm. In comparison with classical technologies, laser processes are generally used for small and medium lot sizes but with strongly increased material and geometric variability (Gillner et al., 2005).

Industrial product parts and components are being made smaller to reduce energy consumption and save space, which creates a growing need for microwelding of thin foil less than 100 μm thick. For this purpose, laser processing is expected to be the method of choice because it allows more precise heat control compared with arc and plasma processing (Abe et al., 2005).

There is a trend toward increased steel microwelding applications in the medical device manufacturing industry; these require spot sizes down to 25 μm and even smaller. Applications include sensors with very thin membranes (where no thermal deformation is allowed), microbonded wires with diameters of about 15 μm and welding of markers on to stents. As medical devices become smaller in size, new challenges will appear that laser welding will have to address (Tolinski, 2008).

Welding with a pulsed Nd:YAG laser system is characterized by periodic heating of the weld pool by an incident high peak power density pulsed laser beam that allow melting and solidification to take place consecutively. The welding speed is defined by the overlap, the pulse repetition rate and the focus diameter. However, due to the very high peak power density involved in pulsed laser welding, the solidification time is shorter than that using a continuous laser or conventional welds. A combination of process parameters such as pulse energy (E_p), pulse duration (t_p), repetition rate (R_r), beam spot size (Φ_b) and welding speed (v) determines the welding mode, i.e., conduction or keyhole (Ion, 2005; Duley, 1999; Steen, 2005).

* Corresponding author. Tel.: +55 18 37431095; fax: +55 18 37422992.
E-mail address: ventrella@dem.feis.unesp.br (V.A. Ventrella).

0924-0136/$ – see front matter © 2010 Elsevier B.V. All rights reserved.
doi:10.1016/j.jmatprotec.2010.06.015

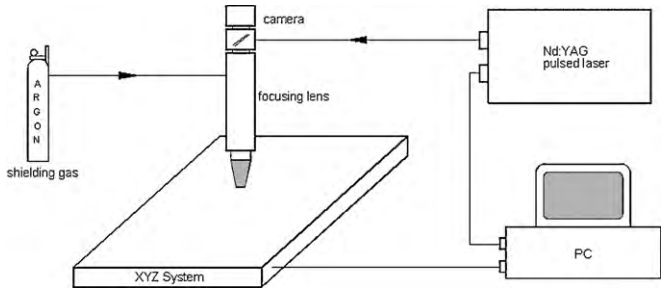

Fig. 1. Schematic of typical pulsed Nd:YAG laser welding system.

Research examining the Nd:YAG laser for continuous welding, pulsed welding, dissimilar sheet welding and coated sheet welding has been published. Kim et al. (2001) reported successful welding of Inconel 600 tubular components of nuclear power plant using a pulsed Nd:YAG laser. Berretta et al. (2007) using a homemade Nd:YAG pulsed laser system studied dissimilar welding of austenitic AISI 304 and martensitic AISI 420 stainless steel. Ping and Molian (2008) utilized a nanosecond pulsed Nd:YAG laser system to weld 60 μm of thin AISI 304 stainless steel foil.

This paper investigates the use of an Nd:YAG laser operating in pulsed mode for welding a 100 μm thick AISI 316L stainless steel thin foil. The effect of pulse energy on weld joint characteristics is studied, and a discontinuity-free welding structure with good mechanical properties is proposed.

2. Experimental apparatus and procedures

This study used a pulsed Nd:YAG laser system. The experimental setup of the laser system is shown in Fig. 1.

AISI 316L was selected as the base metal for welding experiment with the following composition (wt.%): C – 0.03, Cr – 17.28, Ni – 13.0, Mn – 0.80, Si – 0.75, P – 0.045, S – 0.003, and Mo – 2.3. The base material used for this study was thin foil with a thickness of 100 μm. It was cut to a size of 20 mm × 44.5 mm. The experimental results were analyzed on the basis of the relationships between pulse energy and weld bead geometry, the presence of discontinuities and mechanical properties. The specimens were prepared and cleaned to ensure that all samples presented the same surface conditions with a homogeneous finish.

To evaluate the influence of the pulse energy, welding was performed using specimens positioned as lap joints. They were welded with a beam spot size (Φ_b) and beam angle (A_b) of 0.2 mm and 90°, respectively. The focus point was fixed on the surface of the workpiece. The welding speed (v) and repetition rate (R_r) were fixed at 525 mm/min and 39 Hz, respectively. The pulse energy (E_p) varied from 1.0 to 2.25 J at increments of 0.25 J with a 4 ms pulse duration (t_p). Thus, there was one controlled parameter in this process: the pulse energy. The specimens were held firmly using a jig, as shown in Fig. 2, to fixture and prevent absence of contact and excessive distortion. Fixturing is extremely important for thin-section laser welding. Tolerances were held closely to maintain joint fitups without allowing either mismatch or gaps.

The specimens were laser-welded in an argon atmosphere at a flow rate (F_r) of 10 l/min. Back shielding of the joint was not necessary because AISI 316L is not an oxidizable metal like Al and Ti. None of the specimens were subjected to any subsequent form of heat treatment or machining. After welding, the specimens were cut for the tensile shear tests, as shown in Fig. 3. Finally, part of the cut surfaces was prepared for metallographic inspection by polishing and etching to display a bead shape and microstructure. Metallographic samples were prepared by electrolytic etching (2.2 V, 20 s) with a solution of 50% nitric acid. The bead shape measurements were made using an optical microscope with an image analysis system. Fig. 4 shows a schematic illustration of the transverse joint section with the analyzed geometric parameters.

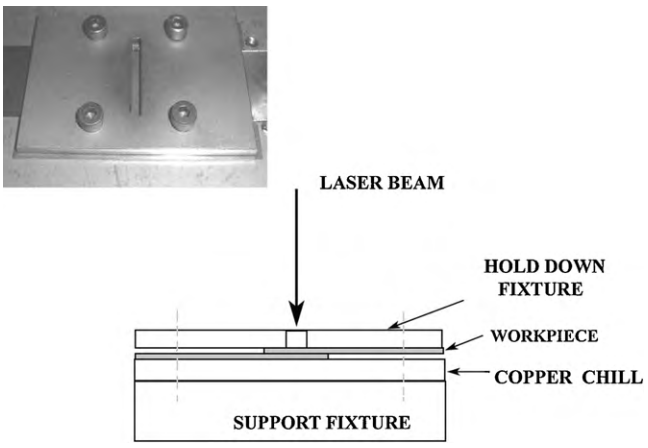

Fig. 2. Schematic of the hold-down fixture developed to hold firmly the thin foils of austenitic stainless steel AISI 316L.

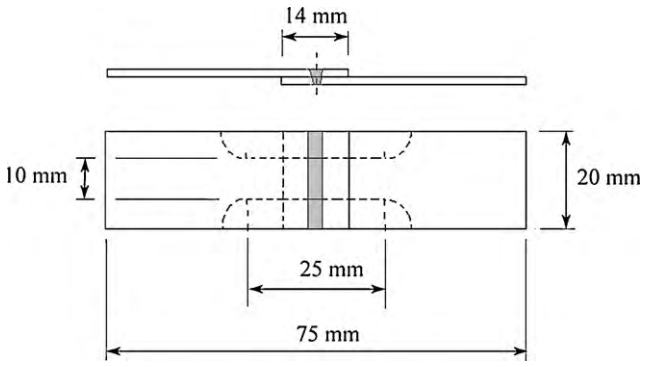

Fig. 3. Lap joint configuration of AISI 316L thin foil and schematic diagram of tensile test specimen design (mm).

The strength of the welds was evaluated using Vickers microhardness and tensile shear strength tests. Microhardness (HV10) tests were performed on a transverse section of the weld bead, parallel to the surface of the thin foils, in the region next to the connection line of the top foil. Microhardness tests identify possible effects of microstructural heterogeneities in the fusion zone and in the base metal. The reported data were the average of five individual results. For the tensile shear test, specimens were extracted from welded samples, and the width of the samples was reduced to 10 mm to lower the load required to fracture them.

3. Results and discussion

The optimum performance of the seam welded joint for chemical seals employed in corrosive environment applications was

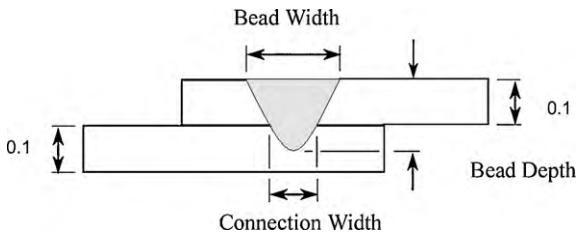

Fig. 4. Schematic of the joint transversal section showing the analyzed geometric parameters (mm).

Please cite this article in press as: Ventrella, V.A., et al., Pulsed Nd:YAG laser seam welding of AISI 316L stainless steel thin foils. J. Mater. Process. Tech. (2010), doi:10.1016/j.jmatprotec.2010.06.015

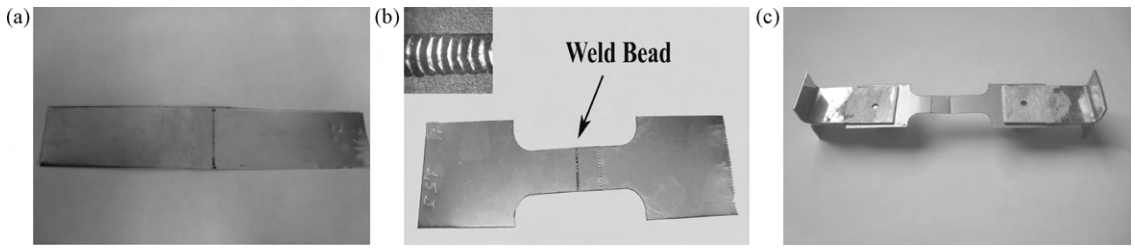

Fig. 5. Top view of welded specimen with 1.5 J pulse energy (a), an external shape of tensile shear test (b) and specimen prepared for the tensile shear test (c).

determined using AISI 316L stainless steel thin foil (100 μm) and an Nd:YAG pulsed laser with different pulse energies (E_p). Fig. 5a shows a top view of a welded specimen (E_p = 1.5 J) and Fig. 5b and c shows the specimen prepared for tensile shear test. It is clearly noticeable in the detail region (Fig. 5b) the no detectable defect existed on the surface of the weld bead or adjacencies. This good surface appearance was observed in specimens welded with pulse energy from 1.0 to 1.75 J. The weld beads showed characteristic of pulsed laser welding. No welding cracks were found in any of the welds; this may be partly due to the good crack resistance of the base metal and the correct welding parameters. No discontinuities were observed in the weld metal. It demonstrates the efficiency of the shielding gas in preventing oxidation, large porosities and gas inclusions. All specimens were laser-welded in the conduction mode: direct heating and energy transmission. The mechanism of direct heating involved absorption of the beam energy by the material surface of the top foil and subsequent transfer of energy into the surrounding material by conduction. The threshold for the formation of a keyhole was observed on the surface of the weld pool at which the laser intensity was highest.

The cross-sectional macrostructures of lap laser welds as a function of pulse energy (E_p) are summarized in Fig. 6. In Fig. 6a and b (specimens with 1.0 and 1.25 J pulse energy, respectively) no penetration at the bottom sheet and no depression at the top of the bead was observed, probably due to insufficient energy to bridge the couple. It is clearly noticeable in Fig. 6a and b the presence of a small gap between couple. The macrostructures showed that melting started at the surface irradiate by the laser beam and the molten pool grew continuously to axial and radial axis. Due to the thin thickness, low pulse energy of the laser beam and the presence of a small gap, the molten pool just grew in the radial direction of the top foil resulting in a no bonded joint with the weld morphology observed in Fig. 6a and b. Depth-to-width ratio of the fusion zone of these specimens was about 0.2. Gaps between foils and gaps in the connection line increase stress and thus are detrimental to weld quality in terms of mechanical properties. As reported in the literature (Kawarito et al., 2007) the presence of wider gaps in welded joints result in more deeply concave underfills. Specimens welded in the present work with low pulse energy, 1.0 and 1.25 J, present no underfill because the molten material did not have enough time to fill the gap. When the pulse energy was increased on the other specimens, a connection region between the foils was observed, as shown in Fig. 6c and d (welded with 1.5 and 1.75 J, respectively). Both specimens present no underfill but an excess of molten material at the root. The penetration depth increased from 133 to 200 μm (full penetration) as the pulse energy increased from 1.5 to 1.75 J. Both joints present an intimate contact between the couples (absence of gap). These specimens present excellent conditions for laser seam welding. In Fig. 6e and f (specimens with 2.0 and 2.25 J pulse energy, respectively), an increase occurred with a depression at the top and a penetration bead. The concavity increased proportionally to the pulse energy (E_p). Moreover, it was evident that specimens welded with 2.0 and 2.25 J pulse energy undergo deformation during joint welding, which causes a large bending moment. Areas near the heat source of the upper foil are heated to higher temperatures and thus expand more than areas away from the heat source or regions of the lower foil. After the foil cools to the initial temperature, the final deformation remains. Like the material heated by the laser beam, the irradiance did not cause the material reach its boiling point; no significant amount of surface material was removed.

The macroscopic examination of the cross sections of all specimens also indicated that the weld pool morphology is essentially

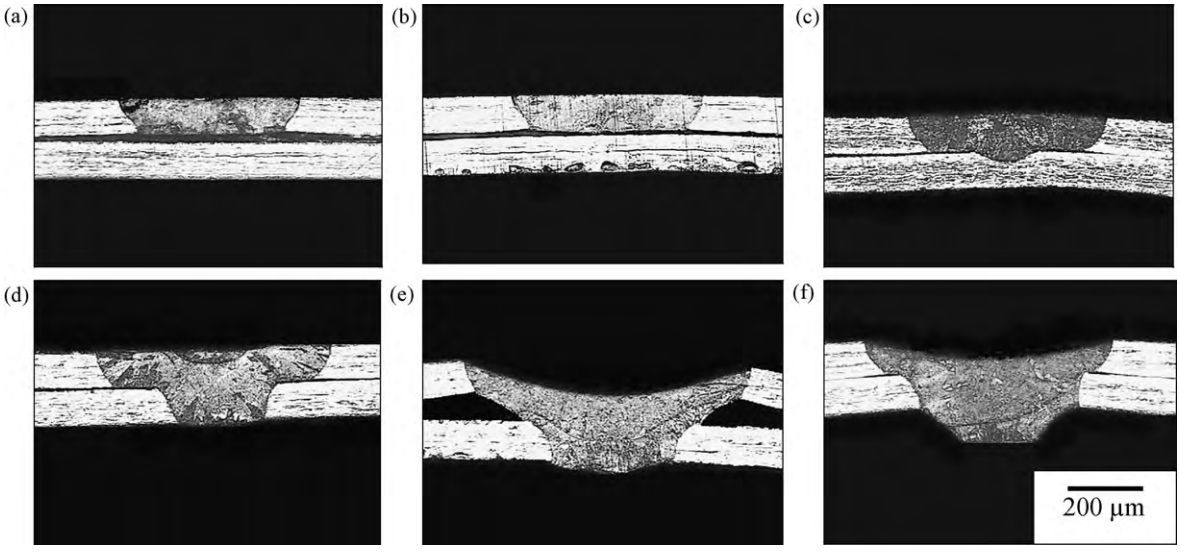

Fig. 6. Cross sections of lap joints made with pulsed Nd:YAG laser welding with different pulse energies. Laser weld parameter: incident angle = 90°, focal position = 0, pulse duration 4 ms and laser energy at: (a) 1.0 J, (b) 1.25 J, (c) 1.50 J, (d) 1.75 J, (e) 2.0 J and (f) 2.25 J. All figures have the same magnification as shown in (f).

Please cite this article in press as: Ventrella, V.A., et al., Pulsed Nd:YAG laser seam welding of AISI 316L stainless steel thin foils. J. Mater. Process. Tech. (2010), doi:10.1016/j.jmatprotec.2010.06.015

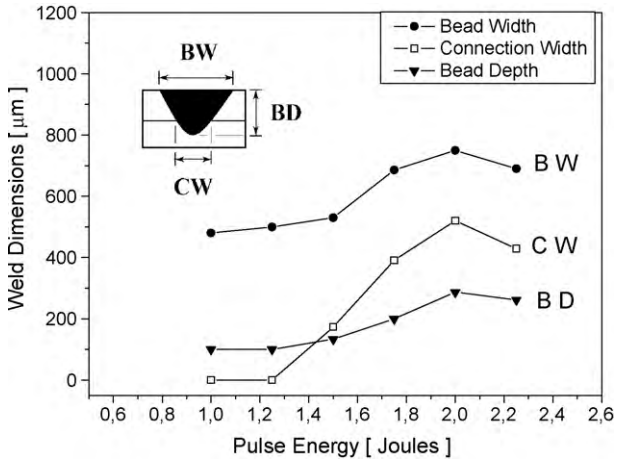

Fig. 7. The effect of pulse energy on the bead width (BD), connection width (CW) and bead depth (BD) of the weld metal.

symmetrical about the axis of the laser beam. A hemispherical weld bead was formed in a similar manner to conventional arc fusion welding processes. This symmetry at the top and bottom was observed in all joints independent of the pulse energy, which suggests a steady fluid flow in the weld pool; however, as the pulse energy increased, a high depression formed at the top.

From the Fig. 6, it can be seen that there exists some influence of pulse energy on the joint geometry, which mainly reflects the change of weld penetration and weld width. When the pulse energy is very low, obvious incomplete penetration appears. As the pulse energy is increased, the weld appearance becomes better. Therefore, when the pulse energy is higher, more volume of the base metal will melt and the welding heat has more time to conduct into the bottom from the top foil and a crater at the top centre was formed due to the vaporization of elements with low melting point.

Liao and Yu (2007) and Manonmani et al. (2007) reported that, in pulsed laser welding with the same incident angle of AISI 304 stainless steel the characteristic lengths of the weld increased as the laser energy increased. The same tendency was observed in the present work as the pulse energy increased to 2.0 J. With pulse energy greater than 2.0 J, excessive burnthrough occurred and an excess of melt material at the root region was observed. This reduced the radial conductive heat transfer at the top foil, and the bead width decreased slightly, as shown in Fig. 6f.

The relationship between pulse energy and weld metal geometry of AISI 316L steel is summarized in Fig. 7. The bead width increased from 480 to 750 μm as pulse energy varied from 1.0 to 2.0 J. This indicated that when the laser beam interacts with the specimen, it creates a liquid melt pool by absorbing the incident radiation. This bead width variation is a result of the higher pulse energy; a high amount of material is molten and then propagates through the base material. In the presence of high pulse energy, part of the melt material passed through the joint, which increased the concavity at the top of the weld, the excess of weld metal at the root and the heat-affected zone extension. On the other hand, at pulse energy of 2.25 J, the molten metal volume decreased, and deep concave underfills occurred. Fig. 6f shows a macrostructure between a fusion zone and base metal in the case of 2.25 J of pulse energy.

These macrostructural results indicate that weld metal characteristics are sensitive to pulse energy variation. To obtain an acceptable weld profile, intimate contact between couples is necessary. The presence of an air gap in the weld joint restringes heat transfer between the workpieces. This results in a lack of fusion of the bottom element or the formation of a hole on the superior element of the joint. As the pulse energy increases, the concavity at the top of the weld and the excess of material at the weld root increase; consequently, the weld joint is weakened. Moreover, higher pulse energy extended the heat-affected zone.

Lack of fusion between couples was observed at pulse energies below 1.5 J. Moreover, lack of fusion between couples was expected to be suppressed by using high pulse energy until the molten pool bridged the gap. The presence of holes was observed at pulse energy above 2.25 J. No welding cracks were observed in any of the welds, which suggests that welding cracks are not sensitive to variations in the pulse energy. Instead, welding cracks are a function of the Cr_{eq}/Ni_{eq} ratio. The presence of spatters, porosities and undercut was not found in the welded joints investigated with optical microscopy.

The HAZ displays the effect of temperature cycling to a peak temperature, T_{max}, which is less than the melting point but may be sufficient to initiate other transformations. The cooling rate of steel, in the HAZ, may approach 1000 °C/s but varies with location, as does T_{max}. The grains in the heat-affected zone were coarsened as the pulse energy (E_p) increased. This phenomenon can be explained by the cooling rate change. An increase in the pulse energy decreased the cooling rate. A slower cooling rate during solidification allowed more time for grain coarsening. In laser welding the heat-affected zones are much narrower than those generated by conventional welding process and are not likely to be sensitized to corrosion.

Analyses of the heat-affected zone (HAZ) showed that it increased as the pulse energy increased. For all tested specimens the top foil HAZ is larger than the bottom foil HAZ, as shown in Fig. 8a and b. This is strongly dependent with the beam energy, conductive heat transfer and with a perfect contact between couple (presence or not of air gap). It is a different processing material with a determined thickness than two foils of the same material with half of the thickness in a lap joint configuration. Air gap acts as

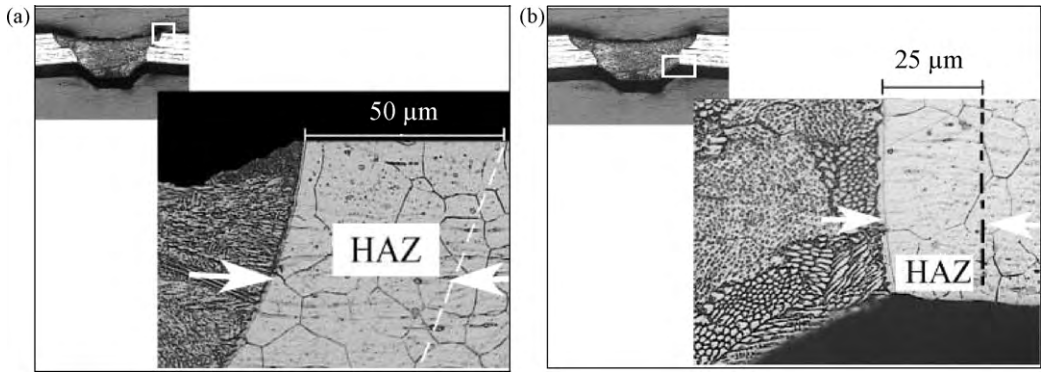

Fig. 8. Microstructure of the specimen welded with 2.25 J. (a) OM photography of heat-affected zone of the top foil and (b) OM photography of heat-affected zone of the bottom foil.

Please cite this article in press as: Ventrella, V.A., et al., Pulsed Nd:YAG laser seam welding of AISI 316L stainless steel thin foils. J. Mater. Process. Tech. (2010), doi:10.1016/j.jmatprotec.2010.06.015

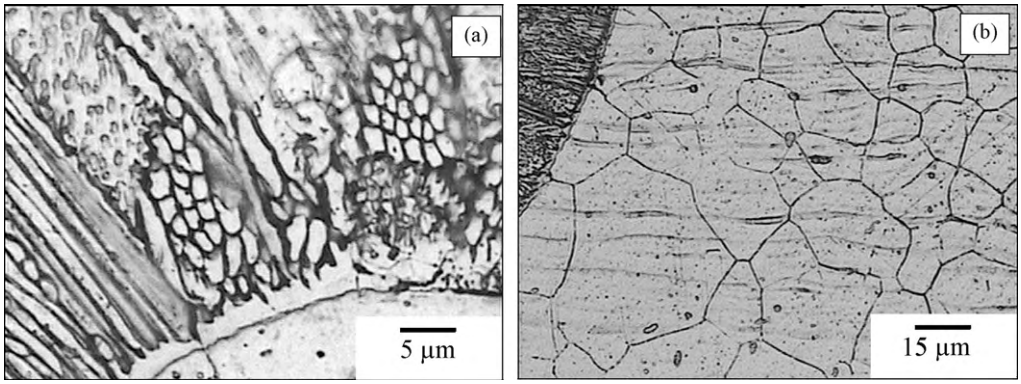

Fig. 9. Typical optical microstructures of the fusion zone (a) and heat-affected zone (b) of an austenitic stainless steel AISI 316L welded joint (2.0 J).

a barrier to heat transfer. In this situation most of the beam energy can be consumed on the side exposed to the laser beam, which results in a large heat-affected zone or bead perforation.

Fig. 8 shows a microscopic examination of the heat-affected zone extension of the top and bottom foils of the specimen welded with 2.25 J. The grains in HAZ are coarsened, and the extension of the heat-affected zone is approximately 50 and 25 μm at the top and bottom foils, respectively. This observation in thin foils seems to contradict the expected narrow heat-affected zone for the laser welding process. The top and bottom HAZ width of the weld becomes obviously larger when the pulse energy (E_p) increases. The HAZ width difference between the top and the bottom becomes smaller as the pulse energy increases, so the cooling rate decreases with increasing pulse energy. Therefore, when the pulse energy is higher, a higher volume of metal is melted and the welding heat has more time to be conducted into the bottom from the top.

Light micrographs of the specimens showed a fine-grained microstructure that is essentially cellular-dendritic in the fusion zone. This type of microstructure is a result of high cooling rates, which are typical of the laser welding process. The formation of a given solidification structure morphology is determined by the G/R ratio (G is the temperature gradient and R is the growth rate) during solidification. Cellular growth structures form rather than dendritic structure if G/R ratio is high (Molian, 1985).

Fig. 9 illustrates typical microstructures of AISI 316L austenitic stainless steel weld joint. Fig. 9a shows the fusion line solidification structure at the top of the weld where the un-melted base metal grains act as substrates for nucleation of the fusion zone columnar grains (epitaxial growth), which are perpendicular to the fusion boundary. Fig. 9b shows the heat-affected zone at the bottom of the joint where the effects of the large thermal gradient in this region are evident. Comparing thin and thick foil welding, it can be concluded that the grains in the solid state coarsen with decreasing parent metal thickness. This shows that the volume of the parent metal plays an important role during the welding thermal cycle. As the material volume decreases, the time to cooling increases and the heat-affected zone appearance coarsens. This indicates that in thin foil welding, heat-affected zone control is of considerable importance for welded joint quality.

First, the failure of all specimens occurs in the region of the parent metal, next to the fusion line of the top foil. This is expected because hardness and tensile strength values are known to be related. The ultimate tensile strength (UTS) tends to increase at first and then decrease as the pulse energy (E_p) increases. The relationship between pulse energy and tensile shear strength of welded joints is summarized in Fig. 10. Specimens welded with a pulse energy lower than 1.5 J were not bonded because the pulse energy was too low, and the molten pool did not have enough time to propagate to the bottom foil; incomplete penetration occurred. Otherwise, when the specimens were welded with pulse energy greater than 1.75 J, excessive underfilling and burnthrough was observed. Perforations in the weld bead were observed with pulse energy higher than 2.25 J. The maximum value of UTS, obtained with a pulse energy of 1.75 J, was up to 95% of the parent metal.

Scanning electron microscopy observations of the welded joint showed that the weld surface region next to the rupture line displayed a sequence of sags due to differential deformations that occur in the weld bead as a result of different microconstituent orientations.

The tensile properties of the welded joint affected by pulse energy (E_p) can be explained by macro and microstructural analyses. When the pulse energy is too low, the welding molten pool has not enough time to form, and incomplete penetration is formed. As the pulse energy increases, the grains in the weld metal and in the HAZ become coarser. The heat-affected zone extension increases too. Discontinuities become more severe. Some precipitates can be present intergranularly and even continuously along the grain boundary. These microstructural changes contribute to a weakness of the weld joint, which reduces the tensile properties as reported in the literature (Quan et al., 2008). Finally, the decrease in the UTS may be related to the change of the microstructures and HAZ extension. Therefore, based on the above analyses it can be concluded that the lower the pulse energy, provided complete penetration occurs, the higher the tensile properties of welded joints.

Hardness profiles of the base metal, heat-affected zone and weld metal of AISI 316L stainless steel thin foils as a function of pulse energy are shown in Fig. 11. No significant difference between hardness of weld metal and the heat-affected zone was obtained; the

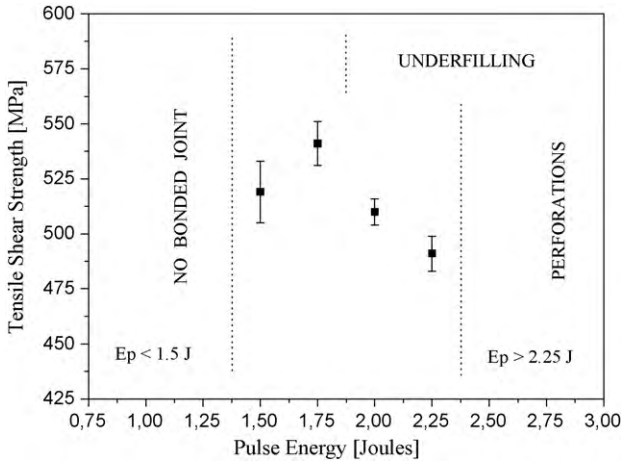

Fig. 10. Tensile shear strength of AISI 316L welded joint at different pulse energies.

Please cite this article in press as: Ventrella, V.A., et al., Pulsed Nd:YAG laser seam welding of AISI 316L stainless steel thin foils. J. Mater. Process. Tech. (2010), doi:10.1016/j.jmatprotec.2010.06.015

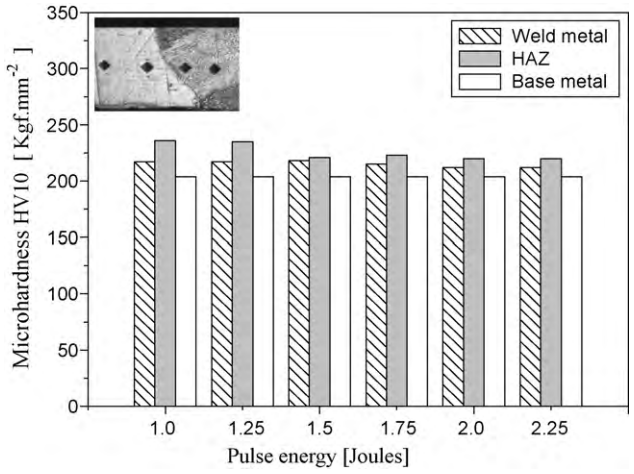

Fig. 11. Hardness profile of base metal, heat-affected zone and weld metal of AISI 316L stainless steel thin foils as a function of pulse energy.

hardness of the heat-affected zone was slightly higher than that of the weld metal regardless of the pulse energy. Base metal hardness was always lower than that of HAZ and weld metal. These results are valid for all joints. This is expected because the mechanical properties of steel, in general, are based on its microstructures (Abdel, 1997).

As can be seen in Fig. 11, the microhardness values (HV10) decreased as the joint energy increased (1.0–2.25 J) to maximum energy (2.25 J). During the solidification of the fusion zone, the material generally loses original strength that is induced by strain hardening. Microhardness profiles in welded joints obtained with lower energy show increasing of the hardness in the fusion zone and a finer microstructure that is induced by rapid cooling.

In summary, the most acceptable weld bead was obtained at a pulse energy of 1.75 J, where the molten pool bridged the couple and the weld bead profile showed minimum underfill and maximum depth (full penetration). The tensile shear test exhibited 541 MPa. No undercut and minimum porosity were observed. No evidence of hot cracking was observed in the weld metal and this is attributed to the rapid solidification conditions typical of the pulsed Nd:YAG laser welding process.

4. Conclusions

The pulsed Nd:YAG laser welding process has been employed to join AISI 316L thin foil. In general, the results obtained from this study demonstrate that is possible to weld 100 μm thickness AISI 316L thin foils, in terms of microstructural and mechanical reliability, by precisely controlling the laser pulse energy. The better performance was due to the high quality joint; a joint marked by full penetration, no underfill and free from microcracks and porosity. This was obtained at an energy pulse of 1.75 J, a repetition rate (R_r) of 39 Hz and a 4 ms pulse duration. This reflects one of the most notable features of pulsed laser welding compared with other processes; welding with low heat input. The work also shows that the process is very sensitive to the gap between couples which prevents good heat transfer between the foils. The shape and dimensions of the thin foil weld bead observed in the present work depended not only on the pulse energy, but also on the presence of gaps between foils. Bead width, connection width and bead depth increased as the pulse energy increased, and then decreased at the end because of burnthrough. The ultimate tensile strength (UTS) of the welded joints initially increased and then decreased as the pulse energy increased. The specimen welded with 1.75 J attained the maximum tensile shear strength. In all the specimens, fracture occurred in the top foil heat-affected zone next to the fusion line. The microhardness was almost uniform across the parent metal, HAZ and weld metal. A slight increase in the fusion zone and heat-affected zone compared to those measured in the base metal was observed. This is related to the microstructural refinement in the fusion zone, induced by rapid cooling.

Acknowledgment

The authors gratefully acknowledge the financial support of CNPq.

References

Abdel, M.B., 1997. Effect of laser parameters on fusion zone shape and solidification structure of austenitic stainless steels. Materials Letters 32, 155–163.
Abe, N., Funada, Y., Imanada, T., Tsukamoto, M., 2005. Microwelding of thin stainless steel foil with a direct diode laser. Transaction of JWRI 34, 19–23.
Berretta, J.R., Rossi, W., Neves, M.D.M., Almeida, I.A., Junior, N.D.V., 2007. Pulsed Nd:YAG laser welding of AISI 304 to AISI 420 stainless steels. Optics and Lasers in Engineering 45, 960–966.
Duley, W.W., 1999. Laser Welding. John Wiley & Sons, New York, pp. 67–94.
Gillner, A., Holtkamp, J., Hartmann, C., Olowinsky, A., Gedicke, J., Klages, K., Bosse, L., Bayer, A., 2005. Laser applications in microtechnology. Journal of Materials Processing Technology 167, 494–498.
Ion, J.C., 2005. Laser Processing of Engineering Materials. Elsevier, Oxford, pp. 327–329, 395–399.
Kawarito, Y., Kito, M., Katayama, S., 2007. In-process monitoring and adaptive control for gap in microbutt welding with pulsed YAG laser. Journal of Physics D: Applied Physics 40, 183–190.
Kim, D.J., Kim, C.J., Chung, C.M., 2001. Repair welding of etched tubular components of nuclear power plant by Nd:YAG laser. Journal of Materials Processing Technology 14, 51–56.
Liao, Y., Yu, M., 2007. Effects of laser beam energy and incident angle on the pulse laser welding of stainless steel thin sheet. Journal of Materials Processing Technology 190, 102–108.
Manonmani, K., Murugan, N., Buvanasekaran, G., 2007. Effects of process parameters on the bead geometry of laser beam butt welded stainless steel sheets. International Journal of Advanced Manufacturing Technology 32, 1125–1133.
Molian, P.A., 1985. Solidification behaviour of laser welded stainless steel. Journal of Materials Science Letters 4, 281–283.
Ping, D., Molian, P., 2008. Q-switch Nd:YAG laser welding of AISI stainless steel foils. Materials Science & Engineering A 486, 680–685.
Quan, Y.J., Chen, Z.H., Gong, X.S., Yu, Z.H., 2008. Effects of heat input on microstructure and tensile properties of laser welded magnesium alloy AZ31. Materials Characterization 59, 1491–1497.
Steen, W.M., 2005. Laser Material Processing, third ed. Springer, London, pp. 160–165.
Tolinski, M., 2008. Lasers seal the deal in medical. Manufacturing Engineering 140, 14–20.

Please cite this article in press as: Ventrella, V.A., et al., Pulsed Nd:YAG laser seam welding of AISI 316L stainless steel thin foils. J. Mater. Process. Tech. (2010), doi:10.1016/j.jmatprotec.2010.06.015